

Structure Determination of the $\text{Si}(111):\text{B}(\sqrt{3}\times\sqrt{3})R30^\circ$ Surface: Subsurface Substitutional Doping

R. L. Headrick, I. K. Robinson, E. Vlieg, and L. C. Feldman

AT&T Bell Laboratories, Murray Hill, New Jersey 07974

(Received 29 March 1989)

Synchrotron x-ray diffraction has been used to analyze the $(\sqrt{3}\times\sqrt{3})R30^\circ$ reconstruction of $\text{B}/\text{Si}(111)$. Excellent agreement is obtained with in-plane data for a model in which boron sits in every third site of threefold symmetry. Out-of-plane diffraction, however, is only consistent with boron *below* the surface in the fivefold-coordinated substitutional site under a silicon T_4 adatom. The structure is confirmed by the growth behavior under room-temperature Si deposition in which the silicon adatom is displaced from its ordered site leaving boron in a two-dimensional ordered substitutional array.

PACS numbers: 68.35.Bs, 61.10.Jv, 68.55.Bd, 68.55.Ln

The word "adsorbate" in surface physics conveys the idea of attachment of a deposited atom *on top* of a surface, while the term "surface alloy" conveys the idea of incorporation into the lattice for miscible atoms. Analogous terms "interstitial" and "substitutional" are used to describe impurity sites at low concentrations in bulk crystals. When an atom is deposited on a substrate in which it is immiscible, it is widely assumed that it will remain as an adatom on top of the substrate. Counterintuitively, we have found here that B adopts a subsurface site on $\text{Si}(111)$, forming a two-dimensional alloy with no three-dimensional analog. This explains why an ordered layer of B can be preserved on $\text{Si}(111)$ after subsequent Si deposition and growth,^{1,2} and why this does not occur for other elements which are true adsorbates.²

Surface x-ray crystallography is now a well established technique for the determination of adsorbate structures as well as reconstructed surfaces.³ It takes advantage of the lower symmetry of the surface that gives diffraction features in positions without contributions from the bulk. Since the diffraction is accurately kinematical, the analysis is unambiguous and straightforward. Originally surface reconstructions were determined in a two-dimensional projection using two-dimensional data only, but more recently this has been extended to three-dimensional surface structures by using the continuous profiles of the structure factors with perpendicular momentum transfer.^{4,5} The main result presented here is completely invisible in two-dimensional data and depends entirely on the out-of-plane intensity variation. Furthermore, we report for the first time crystallographic determinations as a function of coverage during *in situ* deposition.

The x-ray diffraction measurements were carried out at the AT&T X16A beam line of the National Synchrotron Light Source (NSLS) located at Brookhaven National Laboratory, by use of 1.1-Å-wavelength radiation and a four-circle diffractometer.⁶ $\text{Si}(111)$ samples were implanted with boron at 30 keV to 2×10^{16} cm^{-2} followed by annealing at 1050°C for 90 min. The surfaces were prepared by chemical growth of a thin protective

oxide layer before transferring into an ultrahigh-vacuum system attached to the diffractometer. The boron $(\sqrt{3}\times\sqrt{3})R30^\circ$ surface reconstruction (called simply $\sqrt{3}$ below) was prepared by heating the sample to 900°C, desorbing the protective oxide layer, and allowing $\frac{1}{3}$ monolayer of the implanted boron to segregate to the surface.

Data in the form of structure factors $F_{hk}(l)$ were obtained by numerical integration of rocking curves and correcting for the Lorentz factor ($\sin 2\theta$) and active area ($\sin 2\theta$). A hexagonal unit cell⁷ was chosen for $\text{Si}(111)$ with in-plane lattice parameters $a=b=3.84$ Å, and out-of-plane lattice parameter $c=9.41$ Å. The data are divided into two categories: "in-plane" data [$F_{hk}(l)$ near $l=0$] that contain information about the surface structure projected onto the plane of the surface, and intensity profiles of fractional-order rods (h,k discrete and l continuous) that depend on the full three-dimensional configuration of the reconstructed layer. The in-plane data sets consisted of 62 reflections from which 18 inequivalent structure factors were obtained. Of these, 5 were integer-order structure factors. Atomic coordinates and the surface Debye-Waller factor of model structures were refined using a χ^2 minimization.⁸ The errors in the data were derived from the reproducibility of the multiply measured reflections, so that a fit of $\chi^2=1$ represents agreement at the level of the experimental error.

The weak scattering factor of boron implies that it makes a small contribution to the total x-ray intensity for any reflection. Hence, this analysis centers on the direct determination of the Si sites; the B site is then determined subsequently.

First, a data analysis was performed using only the in-plane reflections. The class of structures that give the best overall agreement with the data are those with six surface silicon atoms per $\sqrt{3}$ cell (top double layer, including adatoms) and the in-plane distortions of the surface constrained by the $p31m$ plane group of the $\sqrt{3}$ unit cell. When a threefold axis passes through a second-layer Si [denoted Si(2)], radial displacements are permitted of the top layer [Si(1)] towards or away from this

axis. We found a good fit ($\chi^2=1.28$) with displacements of $0.24 \pm 0.02 \text{ \AA}$ towards the axis. Radial displacements of the in-plane position of the fourth layer are permitted by symmetry, so we have also refined the in-plane position of Si(4). Adding a boron atom over Si(2) lowers χ^2 to 1.19, whereas $\chi^2=1.72$ for a site over the fourth layer and $\chi^2=1.66$ for a site over the first layer. Alternatively, we can introduce symmetric displacements towards the threefold axis passing through Si(4), yielding $\chi^2=1.89$. However, adding boron at this axis increases χ^2 to 2.11. Therefore, we can conclude a *projected* structure with in-plane displacements either towards Si(2), analogous to Si(111)-Ga^{9,10} and Si(111)-Sn,¹¹ or towards the threefold axis passing through Si(4), but find that only the first model favors introducing a boron atom at the center of the displacements. In general, other model surface structures with greater or fewer surface Si atoms give much poorer agreement with the data (typically $\chi^2 \geq 10$). A structure with six surface atoms per $\sqrt{3}$ cell, but a lower plane-group symmetry was recently proposed for this system;¹² this model gives relatively poor agreement with the in-plane data, yielding $\chi^2=2.66$.

The out-of-plane data set consists of the $(\frac{7}{3}, \frac{1}{3})$ and $(\frac{8}{3}, \frac{2}{3})$ rods, which were measured over $l = \pm 1.2$ and $l = \pm 1.4$, respectively. The intensity along the rods is not constant, indicating that the reconstruction is not confined to one layer. Our first attempt was therefore to fit the conventional adatom models.⁹ The calculated fractional-order rods for this refined geometry (Fig. 1) do not reproduce the data properly and give $\chi^2=3.64$. Similarly, the H_3 adatom model [boron over Si(4)] gives a very flat profile and $\chi^2 > 6$ for physically reasonable

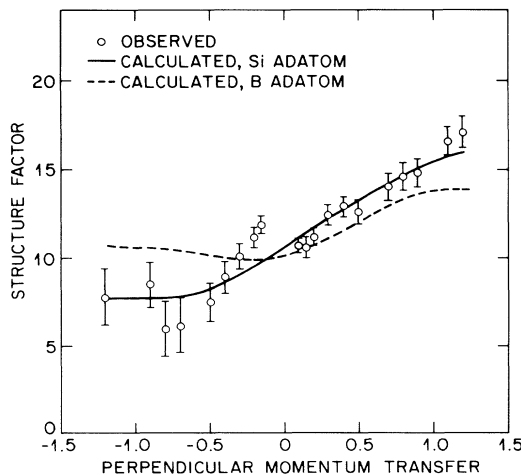


FIG. 1. Perpendicular-momentum-transfer dependence of the $(\frac{7}{3}, \frac{1}{3})$ structure factor. The negative values of l were obtained by applying the center of symmetry to the $(\frac{1}{3}, \frac{7}{3}, l)$ data. Calculated curves are for the best "boron on top" and "silicon on top" T_4 adatom models.

bond lengths and bond angles. Therefore, we conclude that neither of the conventional boron-on-top $\sqrt{3}$ adatom models are consistent with the out-of-plane data.

Much better agreement was obtained by varying the perpendicular positions of Si(2) (starting with the T_4 adatom model) without constraining its bonding. Using the full data set including the out-of-plane as well as the in-plane data, we plotted the variation of χ^2 as a function of two parameters: the z coordinates of Si(2) and B (Fig. 2). The fit is always better when Si(2) is *above* the surface in the T_4 adatom site regardless of the position of the boron atom. The variation of χ^2 as a function of z_B is very small, but the absolute minimum of χ^2 occurs with the boron atom below the surface. However, the position of the boron atom can also be inferred from the *absence* of a silicon atom in a second-layer site under the Si adatom, since it is not physically reasonable to leave this site vacant. We call this site the S_5 site because it is a fivefold-coordinated substitutional site.

With a total of five variable displacements, the optimum model ($\chi^2=1.44$) has $\Delta z_{\text{Si}(1)} = -0.17 \pm 0.20 \text{ \AA}$ and $\Delta r_{\text{Si}(1)} = -0.26 \pm 0.01 \text{ \AA}$ for the first silicon layer. Other displacements from the ideal structure are very small: $\Delta r_{\text{Si}(4)} = -0.02 \pm 0.01 \text{ \AA}$, and $\Delta z_{\text{Si}(2)}, \Delta z_{\text{Si}(4)} < 0.06 \pm 0.20 \text{ \AA}$. We used a value of $B=0.45 \text{ \AA}^2$ for the Debye-Waller factor of bulk Si and $B=1.4 \text{ \AA}^2$ for

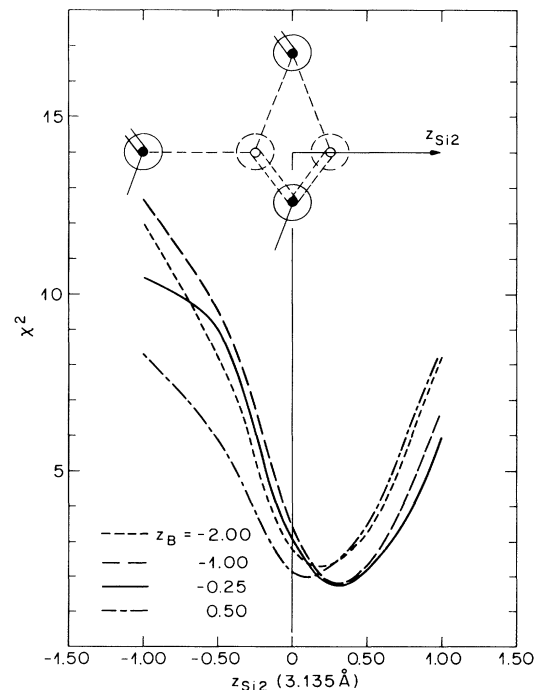


FIG. 2. χ^2 as a function of $z_{\text{Si}(2)}$. A range of values of z_B is shown. Inset: The range of configurations considered on the same abscissa. Sites that are consistent with a Si-Si bond length of 2.35 \AA are indicated by dashed circles. The abscissa is in units of the Si(111) double-layer spacing.

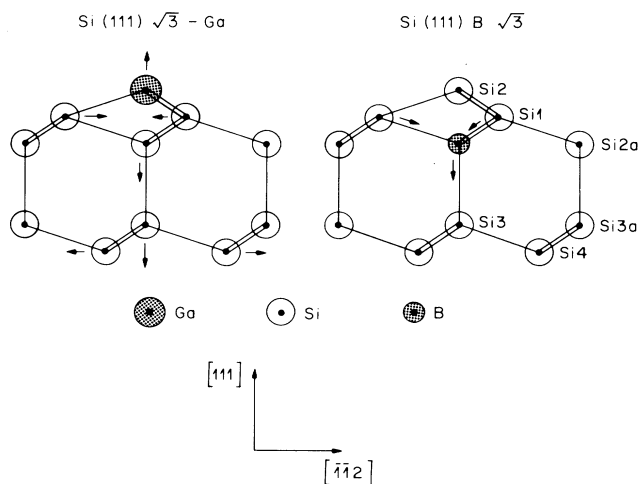


FIG. 3. Model of the Si(111)- $\sqrt{3}$ Ga structure as proposed in Ref. 10 (left). Proposed structure for Si(111):B- $\sqrt{3}$ (right). Arrows indicate the direction of displacements from the ideal tetrahedrally bonded configuration.

boron in this analysis. $B_{\text{Si}(1)}$, $B_{\text{Si}(2)}$, and $B_{\text{Si}(2a)}$ were varied as a single parameter with the constraints $B_{\text{Si}(2)} = 1.5B_{\text{Si}(1)}$ (chosen to qualitatively take into account the expected enhanced vibrational amplitude of the adatom), $B_{\text{Si}(2a)} = B_{\text{Si}(1)}$. The optimum value was $B_{\text{Si}(1)} = 1.6 \pm 0.2 \text{ \AA}^2$. The calculated $(\frac{2}{3}, \frac{1}{3})$ rod intensity profile for this structure is shown in Fig. 1. Figure 3 shows the final structure with the directions of displacements from the ideal undistorted Si-on-top model. All of the Si z coordinates are stable but the boron atom is constrained to sit 2.00 \AA (the sum of covalent radii) above the third-layer Si atom.

The stability of boron in the S_5 subsurface site relative to the T_4 adatom site is likely to be related to relief of subsurface strain by the unique mechanism of substituting a smaller boron atom for silicon. Table I shows the first- and fourth-layer in-plane distortions for the boron $\sqrt{3}$ structure with those of several other Si(111)- and Ge(111)- T_4 adatom reconstructions. We can see from Fig. 3 that for the Si(111)-Ga structure, strain is transferred down to deeper layers because the rigid Si-Si bond cannot be compressed easily. In contrast, the displacements in the B $\sqrt{3}$ reconstruction show a different

TABLE I. Experimentally determined in-plane displacements for Si(111)- and Ge(111)-adsorbate systems.

Reconstruction	$\Delta r_{\text{Si}(1)}$ (\AA)	$\Delta r_{\text{Si}(4)}$ (\AA)	Ref.
Si(111):B-($\sqrt{3} \times \sqrt{3}$)	-0.26(2)	-0.02(1)	Present work
Si(111)-($\sqrt{3} \times \sqrt{3}$)Ga	-0.12	+0.05	10
Si(111)-($\sqrt{3} \times \sqrt{3}$)Sn	-0.21(2)	+0.10(1)	11
Ge(111)-($\sqrt{3} \times \sqrt{3}$)Sn	-0.20(3)	+0.11(1)	4
Ge(111)-($\sqrt{3} \times \sqrt{3}$)Pb	-0.16(3)	+0.07(2)	4

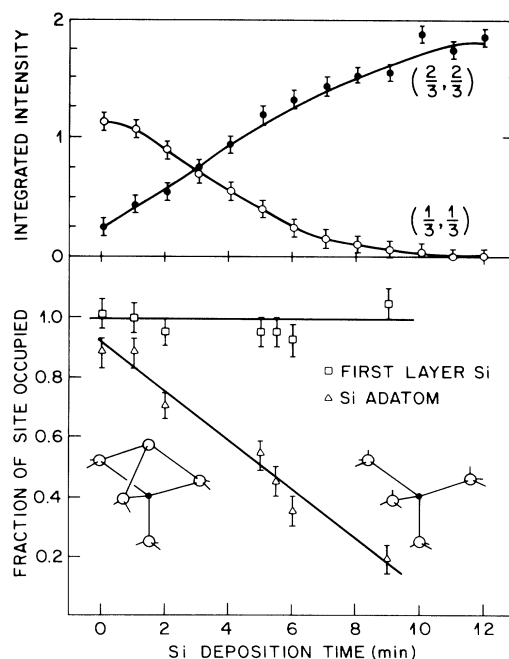


FIG. 4. Coverage dependence of the $(\frac{1}{3}, \frac{1}{3})$ and $(\frac{2}{3}, \frac{2}{3})$ in-plane reflections during Si deposition (upper panel), and of the Si adatom occupancy and first-layer Si occupancy during Si deposition, obtained by crystallographic analysis of in-plane data sets (lower panel). The deposition rate was $\approx 0.25 \text{ \AA}/\text{min}$.

behavior: Although the first-layer in-plane displacement is the largest shown in Table I, the fourth-layer displacement is the smallest.

We have also investigated the Si(111):B- $\sqrt{3}/a$ -Si interface reconstruction by *in situ* x-ray analysis with silicon deposition from a Si source onto the B $\sqrt{3}$ surface with the sample at room temperature. Complete in-plane data sets were collected at a number of coverages between zero and around two monolayers. Figure 4 shows that a transformation between structures takes place since the $(\frac{2}{3}, \frac{2}{3})$ intensity actually increases as the Si coverage is increased.

The entire phenomenon can be explained as systematic removal of the silicon adatom from its ordered site, while leaving the subsurface boron undisturbed. Figure 4 shows the results of three-parameter fits of in-plane data sets as a function of Si coverage. The three parameters are occupancy of the Si(2) adatom site, occupancy of the first-layer Si(1) site, and the in-plane displacement of the first layer [$\Delta r_{\text{Si}(1)}$]. The occupancy represents the probability that the site is filled in the two-dimensional crystal. The agreement of this model with the data was excellent, $\chi^2 = 1.66$ for the worst data point. The Si adatom occupancy decreases linearly with Si deposition time, while the first-layer Si occupancy remains almost constant. The in-plane displacement of the first layer

(not shown) does not change significantly.

The changing adatom occupancy persuades us that the adatom density on the surface changes as a function of Si coverage. Before depositing silicon, the occupancy is ≈ 0.9 , corresponding to 90% of the adatoms on ordered sites. As deposition commences, the occupancy decreases linearly to zero, demonstrating that the Si adatoms are unstable in the presence of excess surface silicon. Disordering of the first complete layer, Si(1), would decrease the occupancy of Si(1); alternately, ordering (i.e., epitaxial growth) of the deposited Si would show up as a systematic *increase* of the Si(1) occupancy because the next layer in the Si stacking sequence is atop Si(1). Figure 4 shows that the occupancy of the first layer, Si(1), remains constant at 1.0, indicating that this layer remains ordered and that the deposited Si does not order. Since the removal of a silicon adatom does not destroy or otherwise alter the $\sqrt{3}$ structure, boron remains on its ordered site at the interface. This is additional strong evidence in favor of the assignment of boron to a subsurface site underneath the Si adatom; for example, if boron did not occupy a site along the same threefold axis as the Si adatom (as proposed in Ref. 12), then the adatom-induced displacements of Si(1) would disappear or change direction when the Si adatom was displaced from its site.

Clean Si(111) adopts the famous 7×7 reconstruction instead of a $\sqrt{3}\times\sqrt{3}$ because the lower density of adatoms provides a compromise between dangling bonds and subsurface strain.¹³ Each Si adatom reduces the number of surface dangling bonds by two so that denser arrangements of them such as 2×2 or $\sqrt{3}\times\sqrt{3}$ have fewer dangling bonds than the 7×7 . The stability of the Si(111):B- $\sqrt{3}$ reconstruction can be qualitatively accounted for by the proposed structure since we have shown experimentally that the subsurface strain is relieved while at the same time the number of dangling bonds is minimized. In addition, each boron atom can accept one electron from adatom dangling bonds, further

reducing the surface energy.

In conclusion, we have shown that the Si(111):B- $\sqrt{3}$ reconstruction consists of a $\sqrt{3}$ array of Si adatoms atop substitutional boron. Overgrowth of Si at room temperature evolves a new interface reconstruction in which the Si adatoms are displaced from ordered sites, but the boron remains ordered.

We thank A. A. McDowell for valuable contributions. The NSLS facility is supported by the U.S. Department of Energy under Grant No. DE-AC02-76CH00016.

¹K. Akimoto, J. Mizuki, I. Hirose, T. Tatsumi, H. Hirayama, N. Aizaki, and J. Matsui, in *Extended Abstracts of the Nineteenth Conference on Solid State Devices and Materials* (Business Center for Academic Societies, Tokyo, 1987), p. 463.

²R. L. Headrick, L. C. Feldman, and I. K. Robinson, *Appl. Phys. Lett.* **55**, 442 (1989).

³I. K. Robinson, in *Handbook of Synchrotron Radiation, Vol. III*, edited by D. E. Moncton and G. S. Brown (North-Holland, Amsterdam, 1989).

⁴J. S. Pedersen, R. Feidenhans'l, M. Nielsen, and K. Kjaer, *Surf. Sci.* **189/190**, 1047 (1987).

⁵M. S. Altman, P. J. Estrup, and I. K. Robinson, *Phys. Rev. B* **38**, 3032 (1988).

⁶P. Fuoss and I. K. Robinson, *Nucl. Instrum. Methods Phys. Res., Sect. A* **222**, 171 (1984).

⁷I. K. Robinson, W. K. Waskiewicz, R. T. Tung, and J. Bohr, *Phys. Rev. Lett.* **57**, 2714 (1986).

⁸P. R. Bevington, *Data Reduction and Error Analysis in the Physical Sciences* (McGraw-Hill, New York, 1969).

⁹J. M. Nicholls, B. Reihl, and J. E. Northrup, *Phys. Rev. B* **35**, 4137 (1987).

¹⁰A. Kawazu and H. Sakama, *Phys. Rev. B* **37**, 2704 (1988).

¹¹K. M. Conway, J. E. Macdonald, C. Norris, E. Vlieg, and J. F. van der Veen (unpublished).

¹²F. Thibaudau, Ph. Dumas, Ph. Mathez, A. Humbert, D. Satti, and F. Salvan, *Surf. Sci.* **211/212**, 148 (1989).

¹³D. Vanderbilt, *Phys. Rev. Lett.* **59**, 1456 (1987); I. K. Robinson, *J. Vac. Sci. Technol. A* **6**, 1966 (1988).